New Journal of Physics
The open-access journal for physics

Transformation-based spherical cloaks designed by an implicit transformation-independent method: theory and optimization

Andrey Novitsky[1], **Cheng-Wei Qiu**[2,3,5] **and Saïd Zouhdi**[4]

[1] Department of Theoretical Physics, Belarusian State University, Nezavisimosti Avenue 4, 220050 Minsk, Belarus

[2] Research Laboratory of Electronics, Massachusetts Institute of Technology, 77 Massachusetts Avenue, Cambridge, MA 02139, USA

[3] Department of Electrical and Computer Engineering, National University of Singapore, 4 Engineering Drive 3, Singapore 117576, Singapore

[4] Laboratoire de Génie Electrique de Paris, SUPELEC, Plateau de Moulon 91192, Gif-sur-Yvette, France

E-mail: eleqc@nus.edu.sg

New Journal of Physics **11** (2009) 113001 (16pp)
Received 25 June 2009
Published 2 November 2009
Online at http://www.njp.org/
doi:10.1088/1367-2630/11/11/113001

Abstract. Based on the concept of the cloak generating function, we propose an implicit transformation-independent method for the required parameters of spherical cloaks without knowing the needed coordinate transformation beforehand. A non-ideal discrete model is used to calculate and optimize the total scattering cross-sections of different profiles of the generating function. A bell-shaped quadratic spherical cloak is found to be the best candidate, which is further optimized by controlling the design parameters involved. Such improved invisibility is steady even when the model is highly discretized.

[5] Author to whom any correspondence should be addressed.

Contents

1. Introduction

Recently, great progress has been made in both the theory of, and experiments on, invisibility cloaks [1]–[4]. Wide applications have been found in the microwave spectrum [5]–[10], optical regime [11]–[16], elastodynamics [17, 18], quantum mechanics [19, 20] and in acoustics [21]–[24]. One approach to achieve an invisibility cloak is to employ transformation optics (TO) to allow electromagnetic waves to be directed around the concealed region and to be smoothly recovered afterwards. The anisotropic parameters of such a cloak are derived from the coordinate transformation. This approach was generalized from the cloaking of thermal conductivity [25] and then widely applied in many other areas, providing new approaches for concealment of passive/active objects [26, 27], invisible to external observation. The fundamental idea is the invariance of Maxwell's equations under a space-deforming transformation if the material properties are altered accordingly; i.e. a specific spatial compression is equivalent to a variation of the material parameters in the flat space. Based on the TO concept, much effort has been devoted to the study of two-dimensional (2D) cloaks (cylindrical [31], elliptical [32] and arbitrary cross-section [33]) due to the simplicity of the numerical simulations. Inspired by the classic spherical cloak [1], the expressions of electromagnetic fields were explicitly presented in terms of spherical Bessel functions via Mie theory [26]. However, this analytical scattering theory for classic spherical cloaks cannot work if the anisotropic ratio (see the original definition in [34]) is anything other than that in [26]. Two solutions to overcome this problem were proposed: (i) multilayers of alternating isotropic layers [35]; and (ii) the discrete model of the inhomogeneous anisotropic shell, in which each layer is radially anisotropic but homogeneous [36]. Then, the spherical invisibility cloak is near-perfect. Another non-TO route to cloaking of a canonical shape is to use a homogeneous anisotropic [28, 29] or isotropic plasmonic [30] coating. However, in this method the effectiveness and properties of the cloak depend on the object to be cloaked, as well as its size, which needs to be small compared to the wavelength. Usually, with TO-based spherical cloaks we need to know the prescribed transformation functions first, and the required parameters can thus be obtained by constructing the explicit transformation matrices. As reported in what follows, there exists an implicit way to derive the needed cloaking parameters, bypassing the traditional procedure mentioned.

In this paper, we propose a new recipe for designing spherical invisibility cloaks, in which we do not need to know or use the coordinate transformation. By virtue of the cloak-generating function, all the parameters a radially anisotropic spherical cloak needs can be determined analytically and uniquely. Nevertheless, the corresponding coordinate transformation can be found by the calculation of those material parameters. Therefore, the traditional way to design a cloak is reversed. In addition, this reversed and implicit transformation-independent method provides us with an easy way to investigate the role of the parametric profiles in achieving invisibility. Certainly, those sets of parameters from various generating functions are ideal, and all should give zero scattering theoretically. However, in actual situations, one has to consider a discrete multilayered model so that the invisibility performance of different generating functions can be distinguished. The general method developed in [36] is adopted to calculate the far-field scattering. Our numerical results reveal that the power quadratic bell-shaped cloak yields the lowest scattering under the same discretization, which is still pronounced when the ideal cloaking shell is highly discretized.

This paper is organized as follows. Section 2 proposes the reversed design method based on the implicit transformation-independent process, from which the spherical cloak's parameters are determined without knowing specific coordinate transformations. Section 3 addresses the bell-shaped profile of the generating function outperforming the others, including the linear one that corresponds to the classical spherical cloak. Section 4 compares different profiles which give rise to bell-shaped profiles. Section 5 discusses the optimization of bell-shaped quadratic cloaks where the steady improvement in invisibility performance is verified.

2. Transformation-independent design method for arbitrary spherical cloaks

We start with the well-known expressions for the relative permittivity and permeability tensors in the physical space transformed from vacuum

$$\bar{\bar{\varepsilon}} = \bar{\bar{J}} \cdot \bar{\bar{J}}^T / \det(\bar{\bar{J}}), \quad \bar{\bar{\mu}} = \bar{\bar{J}} \cdot \bar{\bar{J}}^T / \det(\bar{\bar{J}}), \tag{1}$$

where $\bar{\bar{J}}$ is the Jacobian matrix with elements $J_{ij} = \partial r_i / \partial r'_j$ [7] (i.e. the derivative of the ith transformed coordinate with respect to the jth original coordinate, both of which run from 1 to 3).

We consider that the parameters of the spherical cloak are only dependent upon the radial position of the spherical coordinates, i.e. $(r', \theta, \varphi) \to (r, \theta, \varphi)$. Supposing r' as radial coordinate in virtual (**original**) space and r as that of the physical (**transformed**) space, one concludes that dielectric permittivity and magnetic permeability tensors, in terms of impedance matching, are

$$\bar{\bar{\varepsilon}}(r) = \bar{\bar{\mu}}(r) = \begin{pmatrix} \varepsilon_{\rm r}(r) & 0 & 0 \\ 0 & \varepsilon_{\rm t}(r) & 0 \\ 0 & 0 & \varepsilon_{\rm t}(r) \end{pmatrix} = \begin{pmatrix} \lambda_{\rm r}/\lambda_{\rm t}^2 & 0 & 0 \\ 0 & 1/\lambda_{\rm r} & 0 \\ 0 & 0 & 1/\lambda_{\rm r} \end{pmatrix}, \tag{2}$$

where $\varepsilon_{\rm r}(r)$ and $\varepsilon_{\rm t}(r)$ are the radial and transverse dielectric permittivities (they coincide with the radial and transverse magnetic permeabilities, respectively). Note that equation (2) appeared first in [37]. In the virtual (**original**) space the light propagates in the sphere of vacuum $0 < r' < b$. It is evident that if an *air* sphere is in the vacuum itself, the light goes through it without scattering. After transforming to the physical (**transformed**) space, the initial sphere becomes the spherical layer $a < r < b$ and the light goes through it without impinging on the inner core ($0 < r < a$). So the inner region becomes concealed, while equation (2) determines the permittivity and permeability tensors of such a cloaking shell. The derivation process of equations (1) and (2) can be found in [38].

Dimensionless parameters λ_r and λ_t appear as the Jacobian matrix diagonal elements: λ_r, $\lambda_\theta = \lambda_t$, and $\lambda_\varphi = \lambda_t$. They are defined as

$$\lambda_r = \frac{dr}{dr'}, \qquad \lambda_t = \frac{r}{r'}. \tag{3}$$

From the above expressions we derive a set of equations

$$\frac{dr}{dr'} = \frac{1}{\varepsilon_t(r)}, \qquad \frac{r}{r'} = \frac{1}{\sqrt{\varepsilon_r(r)\varepsilon_t(r)}}. \tag{4}$$

Manipulating equation (4), we arrive at a differential equation to relate radial and transverse permittivities as

$$\frac{d(r\sqrt{\varepsilon_r(r)\varepsilon_t(r)})}{dr} = \varepsilon_t(r). \tag{5}$$

It should be noted that equation (5) is transformation independent, which alone directly displays the expression that dielectric permittivities of a spherical cloak have to satisfy. This approach is an inverse approach. The direct method is to find the dielectric permittivities from a known function of the coordinate transformation. The inverse approach derives the coordinate transformation from the known radial and transverse dielectric permittivities. Equation (5) can be easily integrated:

$$r\sqrt{\varepsilon_t(r)\varepsilon_r(r)} = C + \int_a^r \varepsilon_t(r_1)\, dr_1, \tag{6}$$

where C is the integration constant. The left-hand side of equation (6) is identical to r' as suggested in equation (4). Hence, there are still two boundary conditions to be used. From the first boundary condition ($r' = 0$ at $r = a$) we can determine the integration constant: $C = 0$. From the second boundary condition ($r' = b$ at $r = b$), we obtain the normalization condition for the transverse dielectric permittivity

$$b = \int_a^b \varepsilon_t(r_1)\, dr_1. \tag{7}$$

Therefore we can take any function for the transverse dielectric permittivity normalized according to (7). The radial dielectric permittivity can be found from equation (6). The normalization can be taken into account automatically, if the *cloak generating function* $g(r)$ is introduced. The generating function is defined as follows. It is proportional to the transverse dielectric permittivity, i.e. $g(r) = C_0\varepsilon_t(r)$, where C_0 is a constant. The constant is automatically canceled using the normalization condition (7):

$$C_0 = \frac{1}{b}\int_a^b g(r_1)\, dr_1. \tag{8}$$

Then transverse dielectric permittivity can be presented via the cloak-generating function $g(r)$:

$$\varepsilon_t(r) = \frac{b g(r)}{\int_a^b g(r_1)\, dr_1}. \tag{9}$$

The dimensionless generating function is an *arbitrary* one. The limitations for $g(r)$ are connected to the experimental realization of a cloak, i.e. with the non-infinite values of the permittivities and permeabilities.

Radial dielectric permittivity can be expressed from equation (6) as

$$\varepsilon_{\mathrm{r}} = \frac{b\left(\int_a^r g(r_1)\,\mathrm{d}r_1\right)^2}{r^2 g(r)\int_a^b g(r_1)\,\mathrm{d}r_1}. \tag{10}$$

We will further classify spherical cloaks in terms of the generating function $g(r)$. Pendry's classic spherical cloak corresponds to the constant generating function $g(r)=1$: substituting $g(r)=1$ into equations (9) and (10) one can easily derive transverse dielectric permittivity $\varepsilon_{\mathrm{t}} = b/(b-a)$ and radial dielectric permittivity $\varepsilon_{\mathrm{r}} = b(r-a)^2/r^2(b-a)$. There are many nontrivial cloak designs, e.g. linear, quadratic, cubic, sinusoidal, etc, some of which will be studied in this paper.

3. Bell-shaped generating function for cloak optimization

Starting from this section we consider non-ideal cloaks since we use a discrete model to compute and compare the far-field scattering. If ideal cloaks are considered, each of the cloak designs is equivalent, leading to zero scattering. Realistic cloaks can be made of multiple homogeneous spherical layers, which replace the inhomogeneous cloaking shell. In this case, the scattering is not zero, but noticeably reduced, and such a cloak realization is called non-ideal (see figure 1). In this section, we will find the best non-ideal cloak, providing the lowest cross-section among all the designs investigated.

We will consider some typical generating functions (for transverse dielectric permittivities) which exhibit different types of profiles. The simplest generating functions are constant, linear and quadratic ones. Which of them provides the best cloaking performance?

The constant generating function produces the dielectric permittivities of Pendry's classic spherical cloak as has been demonstrated in the previous section. The linear generating function can be generally written as $g(r)=r-p$, where p is a constant parameter. In this case, the transverse (9) and radial (10) dielectric permittivities become

$$\varepsilon_{\mathrm{t}}(r) = \frac{2b(r-p)}{(b-a)(b+a-2p)}, \tag{11}$$

$$\varepsilon_{\mathrm{r}} = \frac{b(r-a)^2(r+a-2p)^2}{2r^2(r-p)(b-a)(b+a-2p)}. \tag{12}$$

Parameter p can take any value except $(a+b)/2$. It controls the slope of the transverse permittivity function. If $p<(a+b)/2$, $\varepsilon_{\mathrm{t}}(r)$ increases linearly, and otherwise it decreases monotonically.

The quadratic generating function has the general form $g(r)=(r-p)(r-d)+s$, where p, d and s are tunable parameters. The expressions for the permittivities in the quadratic case can be deduced as

$$\varepsilon_{\mathrm{t}}(r) = \frac{b[(r-p)(r-d)+s]}{P(b)}, \tag{13}$$

$$\varepsilon_{\mathrm{r}} = \frac{bP^2(r)}{r^2[(r-p)(r-d)+s]P(b)}, \tag{14}$$

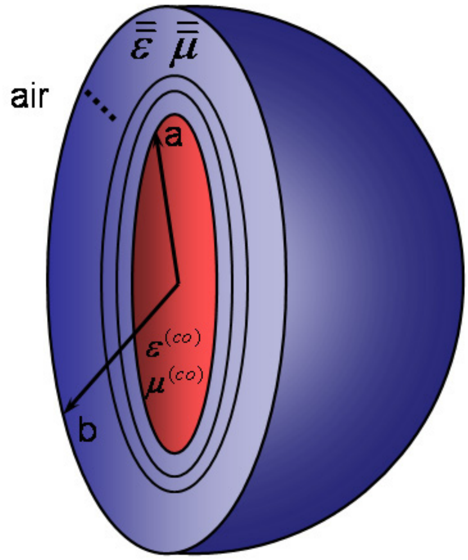

Figure 1. Illustration of the cloaking shell covering the object to be concealed. We consider the spherical cloak in free space with the inner radius $k_0 a = \pi$ and the outer radius $k_0 b = 2\pi$. The core material is glass ($\varepsilon^{(\mathrm{co})} = 1.45^2$ and $\mu^{(\mathrm{co})} = 1$). These quantities are used throughout the whole paper. The material parameters $\bar{\bar{\varepsilon}}$ and $\bar{\bar{\mu}}$ are determined by applying the proposed implicit transformation-independent method to an arbitrary cloak-generating function. The cloaking shell is divided equally into N layers (each layer is homogeneous and anisotropic), and the scattering theory in [36] is used to compute the far-field diagrams.

where

$$P(r) = \frac{r^3 - a^3}{3} - (p+d)\frac{r^2 - a^2}{2} + (pd + s)(r - a). \tag{15}$$

The quadratic transverse permittivity is a parabola when represented by a graph. The parabola can have a minimum (i.e. $s > s_0$) or maximum (i.e. $s < s_0$), where $s_0 = -(b^2 + ab + a^2)/3 + (p + d)(a + b)/2 - pd$.

Using these generating functions, some typical situations depicted in figure 2 are presented. Profile 5 demonstrates the permittivities for the constant generating function $g(r) = 1$ corresponding to Pendry's cloak. Linear generating functions are presented in Profile 4 ($g(r) = r - a$) and Profile 6 ($g(r) = r - b$). The other profiles are produced using quadratic generating functions.

The performances of different cloaks can be compared in terms of their scattering cross-sections. The best cloaking design possesses the lowest cross-section because of the reduced interaction of the electromagnetic wave with the spherical particle. The inhomogeneous anisotropic spherical cloaking shell is divided into N homogeneous anisotropic spherical layers. An experimental realization of this multilayer cloak can be the sputtering onto the spherical core. Throughout the whole paper we use $N = 30$.

In figure 3, the total scattering cross-sections resulting from different generating functions are shown. The definitions of the scattering cross-sections are given in the appendix. Detailed

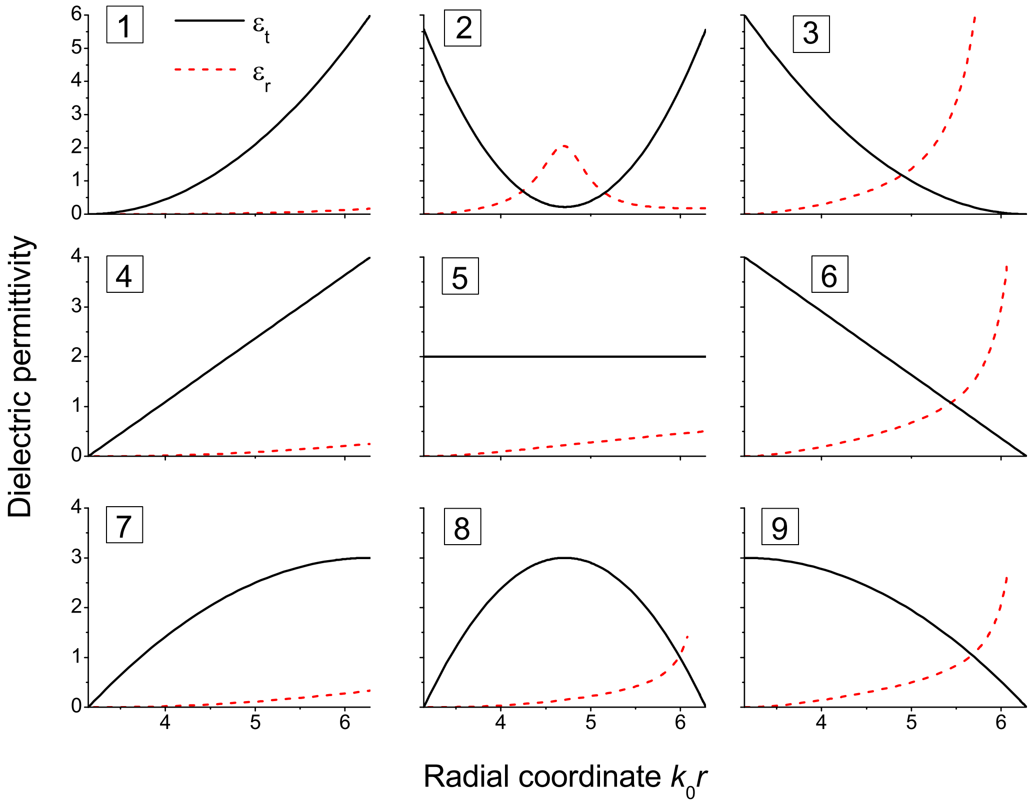

Figure 2. Transverse ε_t and radial ε_r dielectric permittivities corresponding to different profiles of generating function. Profiles 1–9 are described as follows: (1) quadratic generating function with $p = 0$, $d = b$, $s = b^2/4$; (2) quadratic generating function with $p = a$, $d = b$, $s = (b - a)^2/4 + 0.1$; (3) quadratic generating function with $p = a$, $d = 2b - a$, $s = (b - a)^2$; (4) linear generating function with $p = a$; (5) constant generating function; (6) linear generating function with $p = b$; (7) quadratic generating function with $p = a$, $d = 2b - a$, $s = 0$; (8) quadratic generating function with $p = a$, $d = b$, $s = 0$; and (9) quadratic generating function with $p = 0$, $d = b$, $s = 0$.

information on the computational algorithm can be found in [36, 39]. In figure 3, some profiles are approximately equivalent, for example, 1–3, or 4 and 6, or 7 and 9. Profiles 1–3 are characterized by concave-up transverse dielectric permittivity $\varepsilon_t'' > 0$. According to figure 3 they give rise to the worst results. The flat-curvature profiles 4–6 characterized by $\varepsilon_t'' = 0$ are much better. Pendry's cloak (number 5) stands out against the other zero-curvature profiles. However, the most effective cloak design is the case where concave-down transverse permittivity $\varepsilon_t'' < 0$. Profiles 7–9 are better than profiles 4–6, respectively, by approximately 4.8 dB. The quadratic cloak with concave-down transverse permittivity is shown to be the best candidate.

The maximum of ε_t in profile 8 is in the middle position of the cloaking shell. Shifting the maximum of such a bell shape towards the limit at the outer boundary (i.e. profile 7) or inner boundary (i.e. profile 9), the cloaking performance is monotonically degraded as shown in figure 3. If parameter s is extremely large in the quadratic generating function ($s \to \infty$), the

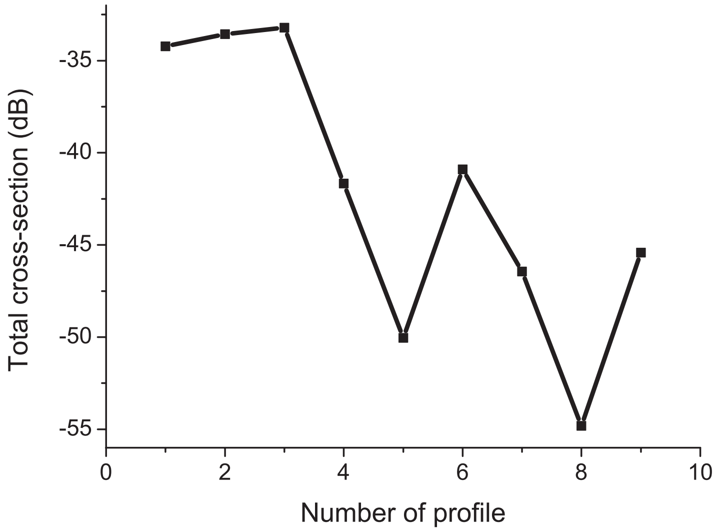

Figure 3. Total scattering cross-sections for profiles of permittivities shown in figure 2. The number of discrete layers forming the cloak equals $N = 30$.

cloak permittivities coincide with those of Pendry's cloak. Thus, the increase of s improves cloak 2 and degrades cloak 8.

The approach proposed to find the cloak which interacts less with the incidence is not undertaken from a strictly mathematical point of view. However, it is simple and robust enough to take into account the significance of the cloak's profile shapes. We suppose that one of the reasons that the quadratic generating function provides the best performance is discretization into layers of equal thickness. It is possible that another type of discretization will correspond with another cloak shape with minimal interaction.

4. The general class of bell-shaped cloaks

From the previous section, it is concluded that the bell-shaped profile of the transverse dielectric permittivity leads to the optimal non-ideal cloaking performance. In the present section, we will consider the general class of bell-shaped cloaks and choose the best type.

Apart from the quadratic cloak, another three simple bell-shaped profiles will be considered: Gaussian, Lorentzian and Sech. All of them have a single parameter T, which sets the width of the profile. We take the maxima of such transverse permittivities in the middle of the cloaking shell region (at the point $(a+b)/2$) to compare with the quadratic cloak.

The Gaussian cloak has the generating function $g(r) = \exp[-(r-(a+b)/2)^2/(4T^2)]$. The permittivity functions are

$$\begin{aligned} \varepsilon_{\mathrm{t}} &= \frac{b}{2\sqrt{\pi}T\,\mathrm{Erf}[(b-a)/(4T)]}\mathrm{e}^{-[(r-(a+b)/2)^2/4T^2]}, \\ \varepsilon_{\mathrm{r}} &= \frac{\sqrt{\pi}Tb\,(\mathrm{Erf}[(b+a-2r)/(4T)]-\mathrm{Erf}[(b-a)/(4T)])^2}{2r^2\,\mathrm{Erf}[(b-a)/(4T)]}\mathrm{e}^{[(r-(a+b)/2)^2/4T^2]}. \end{aligned} \tag{16}$$

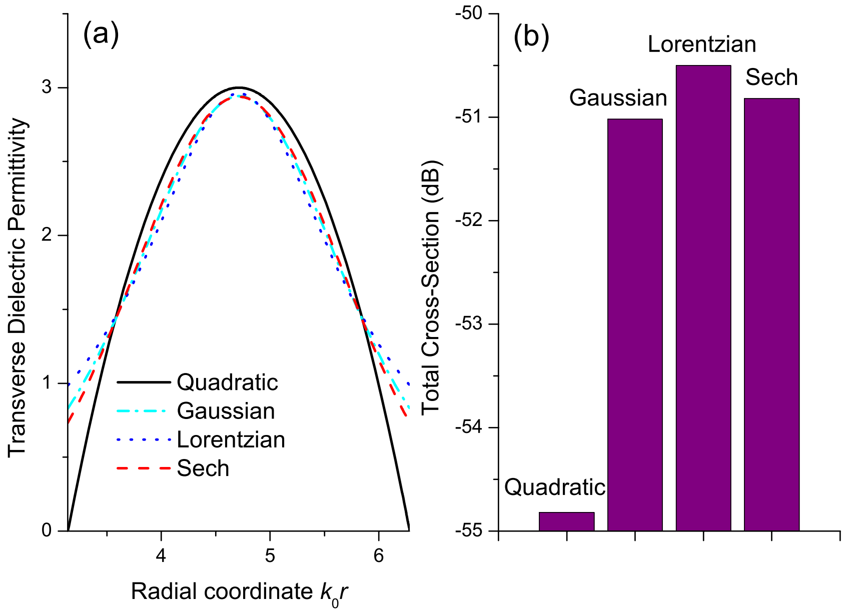

Figure 4. (a) Profiles of transverse dielectric permittivity for quadratic (profile No. 8 in figure 2), Gaussian, Lorentzian and Sech cloaks and (b) total cross-sections of these cloaks. Parameter T equals $(b-a)/4\sqrt{2\ln 2}$ for Gaussian, $(b-a)/(2\sqrt{2})$ for Lorentzian and $(b-a)/(2\sqrt{2}\ln(\sqrt{2}+1))$ Sech cloaks. The number of discrete layers forming each cloak equals $N = 30$.

The generating function of the Lorentzian cloak is $g(r) = 1/[1+(r-(a+b)/2)^2/T^2]$. The transverse and radial permittivities for this cloak are of the form

$$\varepsilon_{\mathrm{t}} = \frac{b}{2T[1+(r-(a+b)/2)^2/T^2]\arctan[(b-a)/(2T)]},$$
$$\varepsilon_{\mathrm{r}} = \frac{Tb(\arctan[(b+a-2r)/(2\,T)]-\arctan[(b-a)/(2\,T)])^2}{2r^2\arctan[(b-a)/(2\,T)]} \times \left(1+\frac{(r-(a+b)/2)^2}{T^2}\right). \tag{17}$$

The Sech cloak generating function depends on the radial coordinate as $g(r) = \mathrm{sech}^2[(r-(a+b)/2)/T]$. The permittivities are as follows:

$$\varepsilon_{\mathrm{t}} = \frac{b\,\mathrm{sech}^2[(r-(a+b)/2)/T]}{2\,T\,\tanh[(b-a)/(2T)]},$$
$$\varepsilon_{\mathrm{r}} = \frac{Tb(\tanh[(2r-b-a)/(2\,T)]-\tanh[(b-a)/(2\,T)])^2}{2r^2\,\mathrm{sech}^2[(r-(a+b)/2)/T]\tanh[(b-a)/(2T)]}. \tag{18}$$

We choose equal 3 dB bandwidths for various transverse permittivity profiles to compare different cloaks. The parameters T that are tuned to provide identical 3 dB bandwidth for each cloak are given in the caption of figure 4. In this figure, we show the total cross-sections of quadratic, Gaussian, Lorentzian and Sech cloaks. Profiles of Gaussian, Lorentzian and Sech

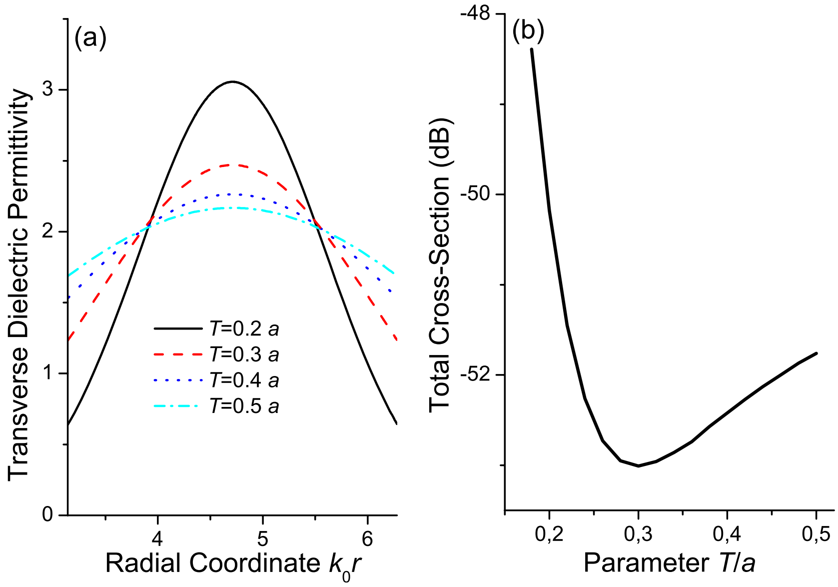

Figure 5. (a) Profiles of transverse dielectric permittivity for Gaussian cloaks with different parameters T and (b) total cross-sections versus parameter T. The number of discrete layers forming the cloak equals $N = 30$.

cloaks are very closely aligned, resulting in similar scattering cross-sections. The influence of permittivity functions on cloak performance is difficult to measure among these three cloaks. However, it is shown that the quadratic cloak in figure 4 provides better invisibility when its transverse permittivity vanishes at the inner and outer boundaries of the cloaking shell.

Since the shapes of the Gaussian, Lorentzian and Sech cloaks are similar, we can just select one of them (e.g. Gaussian) to investigate the significance of the profile, which can be varied by the parameter T. The results are demonstrated in figure 5. The total cross-section has a minimum, but this does not provide better cloaking than the quadratic. The cross-section minimization is achieved approximately at $T = 0.3a$. This profile is shown in figure 5(a), along with profiles for other T parameters. According to this figure the minimization profile has a 3 dB bandwidth equal to $(b - a)/2$. Such a profile is neither too narrow nor too wide because narrow profiles ($T \to 0$) need extremely high discretization and wide profiles ($T \to \infty$) tend toward the limit of Pendry's cloak as shown in figure 5(b). It should be noted that cloaks with narrow profiles interact more strongly than the Pendry cloak, and we conclude that bell-shaped cloaks provide the best results only when appropriately wide.

Thus the bell-shaped quadratic cloak is preferred for non-ideal cloak design, having the lowest cross-section among all the bell-shaped cloaks considered in this section. The near fields of the Pendry (classic) cloak and the quadratic cloak are compared in figure 6. For the quadratic cloak, the intensity of the field is concentrated in the center of the cloaking shell, because the transverse permittivity and permeability become maximal therein. Although the near fields of the discretized Pendry and quadratic spherical cloaks seem similar (they should be), there is still some distinction between the two kinds, i.e. the field intensity of the quadratic spherical cloak (figure 6(b)) is more squeezed and concentrated in the intermediate region of the shell furthest from the core. Therefore it leads to less interaction with the core compared to the pattern of figure 6(a) in which high field intensity is seen more close to and inside the inner core. This

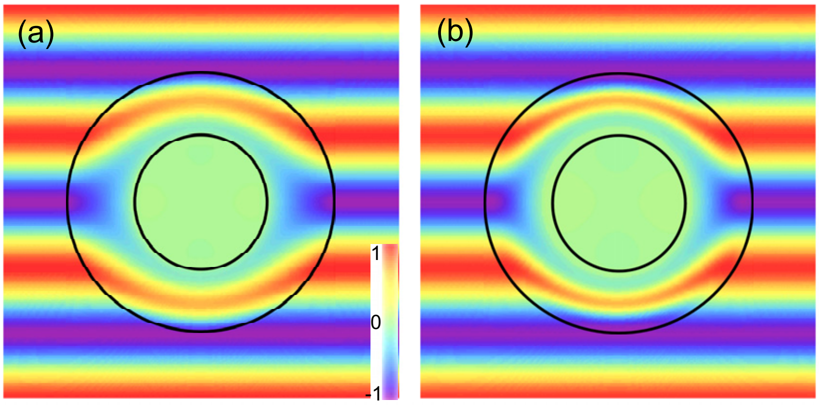

Figure 6. Real part of electric field scattered by (a) Pendry's and (b) quadratic cloaks. The incident plane wave moves from bottom to the top. Parameters: $k_0 a = \pi$, $k_0 b = 2\pi$, $N = 30$. The inner core is filled with glass whose refractive index is 1.45.

results in an improvement in radar cross-section (RCS) reduction in the far field of quadratic spherical cloaks under the same discretization applied to classical linear spherical cloaks. In the following section, we will show how the quadratic cloak results can be improved.

5. Improved quadratic cloaks

The quadratic cloak is characterized by a very simple profile of the transverse dielectric permittivity. Also, the quadratic cloak has a scattering almost 5 dB lower than that of the classical spherical one. Our aim in this section is to find a way of creating high-performance cloaks based on the implicit transformation-independent design method and the bell-shaped quadratic cloak. The high-performance cloak should be similar to the quadratic one. Transverse permittivity should have a maximum and vanish at the inner and outer radii of the shell: $\varepsilon_t(a) = \varepsilon_t(b) = 0$. These properties can be satisfied for the general generating function of the form

$$g(r) = (r-a)(r-b)g_1(r). \tag{19}$$

By choosing function $g_1(r)$, we can set the permittivity profile of the cloak. The function $g_1(r)$ can take arbitrary values at the cloak edges $r = a$ and b, although it should provide the maximum of the transverse permittivity. At first we will consider the maximum at the center of the cloak $r = (a+b)/2$, and then the effect of the non-central maximum position will be studied. For instance function $g_1(r)$ can be selected with a Gaussian profile. Then the cloak can be called Gaussian-quadratic. However, such a design is worse than the simple quadratic shape. To provide a better design we will focus the quadratic dependence using the $g_1(r)$ function

$$g_1(r) = ((r-p)(r-d) + (d-p)^2/4 + s)^n. \tag{20}$$

When $n = 0$, it is the bell-shaped quadratic cloak already discussed. The permittivities at $n > 0$ are suppressed due to lengthy expressions.

In the generating function set by equations (19) and (20), we can vary the power term n (the curvature of the transverse permittivity profile at peak), parameters s (the deviation from

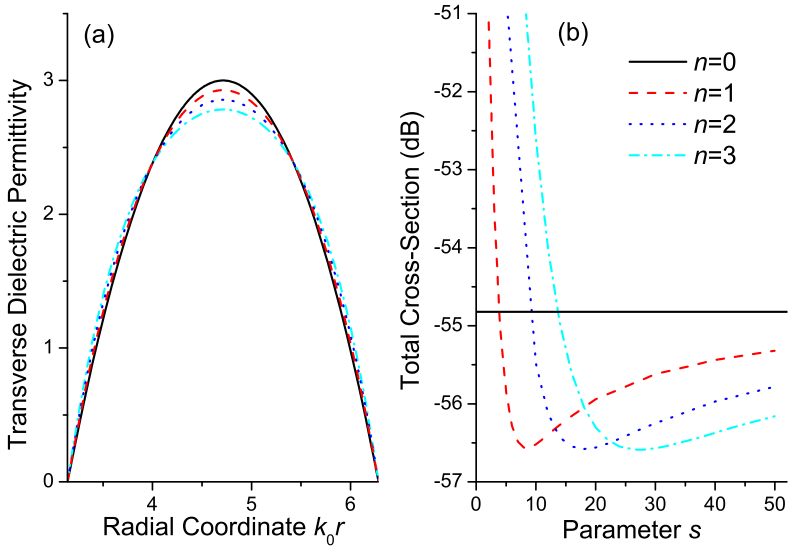

Figure 7. (a) Profiles of transverse permittivity for power quadratic cloaks ($s = 18$) and (b) total cross-sections of these cloaks versus parameter s. Parameters: $p = a$, $d = b$ and $N = 30$. In (b), only $s > 0$ is considered for cloaking purposes because the total cross-sections corresponding to $s < 0$ are significantly larger.

the quadratic cloak) and d (the deviation of the permittivity peak from the center of the cloaking region). At $n = 0$ the generating function is independent of s and d, so the total cross-section is the straight line in figure 7 (the solid line), where the other positive values of n are shown as well. The minima of the cross-sections (the best cloaking performance) occurs for parameter s at approximately $s_{\min} \approx 9n$, i.e. linear to the power n. For a larger s parameter, the curves tend toward the cross-section of the quadratic cloak. For a small and negative s, the shape of the transverse permittivity may contain the minimum and a couple of maxima, therefore the total cross-section is substantially increased. In figure 7(b), the cloaking performance is obviously improved when compared to the quadratic cloak. Let us further study the effect of the peak position of the profile, which is controlled by the parameter d.

The case $d = b$ indicates that the position of the permittivity maximum is in the center of the cloaking shell region. If $d < b$ ($d > b$), the maximum is shifted toward the outer (inner) radius of the cloaking shell. Figure 8 shows that the central position of the permittivity maximum is not the optimal choice. The minimization of the cross-section is achieved for $d \approx 0.84b$. This non-central position is expected as a result of the spherically curvilinear geometry of the cloak.

The improved power performance of the quadratic cloak is notable: the total cross-section is further decreased from -54.84 to -57.52 dB. The improvement is caused by the shape of the profile. The profile should be parabolic-like with a slightly deformed shape.

It is also important to consider the differential cross-sections which provide the scattering intensity at an arbitrary angle. In figure 9, we show the differential cross-sections for some typical cloaking designs designed by the implicit transformation-independent method and considered in a non-ideal situation. The common feature of the cloaks is reduced backscattering. It is seen that the classic spherical cloak is the most visible one. The quadratic cloak (blue dotted

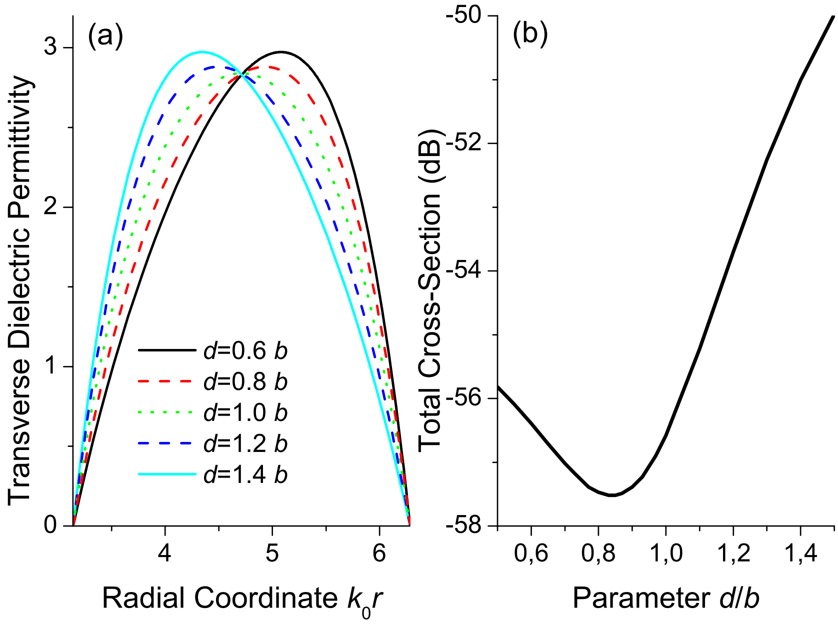

Figure 8. (a) Profiles of transverse dielectric permittivity for power quadratic cloaks and (b) total cross-sections of these cloaks versus parameter d. Parameters: $p = a$, $n = 2$, $s = 18$ and $N = 30$.

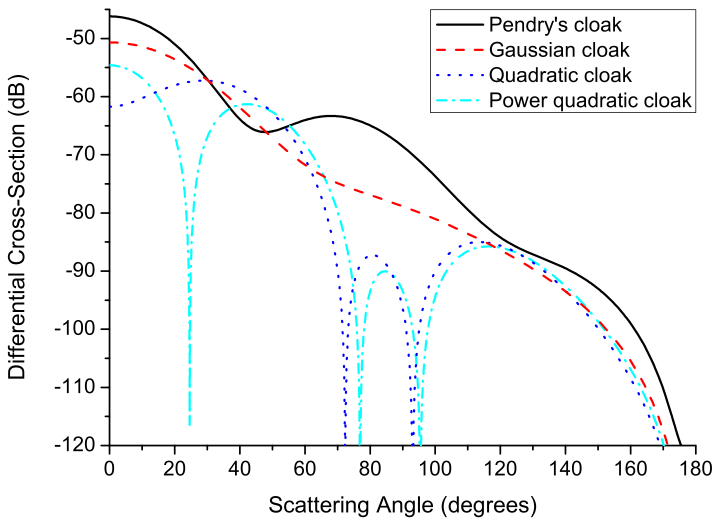

Figure 9. Differential cross-sections for the cloaks derived by the proposed implicit transformation-independent method. The cloak parameters of each given design have been selected to provide the best performance. Parameters: $T = 0.3a$ for Gaussian cloak; $s = 18$, $n = 2$, $p = a$ and $d = 0.84b$ for power quadratic cloak; $N = 30$.

line) can provide much lower scattering over almost all angles compared to Pendry's and the Gaussian bell-shaped cloak. The power quadratic cloak reduces further the scattering for the quadratic cloak near the forward direction.

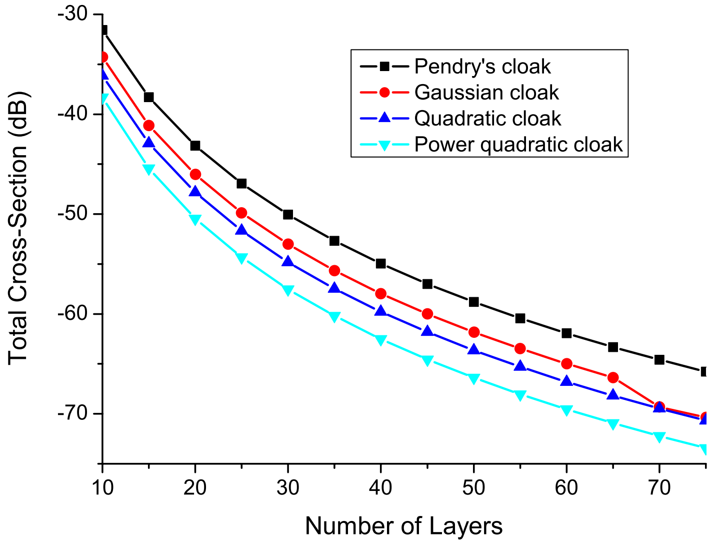

Figure 10. Total cross-sections of different cloak designs versus the number of spherical layers N. The parameters of the cloaks are the same as those in figure 9.

However, one may question whether our non-ideal situation may approach the ideal case when the discretization is high (i.e. N is much larger than 30). If so, each cloak derived from our proposed reversed algorithm should become increasingly identical. Theoretically, it is true that provided $N \to \infty$, the scattering patterns of different profiles should be very close to each other, while the influence of the discretization number N on the optimization result is still of significant importance in practice as shown in figure 10. If N is a small number (e.g. $N = 10$), the continuously varying profile is very roughly approximated by the discretized system, therefore the scattering is great. If the number of layers is large, the discretized structure is very close to the ideal cloaking profile. That is why the scattering in this case is reduced (see the calculated total scattering cross-sections in figure 10). In general, we maintain our conclusions on the optimization for $N = 30$, except for that the performance of the Gaussian cloak matches that of the quadratic cloak at $N = 70$. When N is small, there is a nonlinear dependence of scattering reduction on the value of N. When N is greatly increased the curves become mostly linear as shown in figure 10.

6. Conclusion

We have proposed an implicit transformation-independent method to obtain the required parameters for a spherical cloak, based on the concept of the cloaking generating function. It has been found that the bell-shaped cloaks provide the smallest interaction of the cloaking shell with the electromagnetic radiation under the non-ideal situation (i.e. the cloaking shell is discretized into N layers). Among the bell-shaped cloaks, we have compared quadratic, Gaussian, Lorentzian and Sech cloaks. The last three are very similar in profile shape and in their dependence on the controlling parameters. We have concluded that the best performance is achieved under the bell-shaped transverse permittivity profiles, which vanish at the inner and outer radii of the cloaking shell. The simplest such design is the quadratic cloak. Improved invisibility performance can be provided by the power quadratic cloak with the maximum of the permittivity profile slightly shifted towards the outer boundary. The decrease in the cloak's overall scattering is about 7.5 dB compared to the classical Pendry design, and the improvement is steady even when the discretization N is quite high.

Acknowledgments

This research was supported by the European Network of Excellence 'METAMORPHOSE'. AN acknowledges the Basic Research Foundation of Belarus (F08MS-06). We also thank Professors John Joannopoulos and Steven Johnson for their stimulating comments and revisions throughout the manuscript preparation.

Appendix. Scattered field calculation

We have used the matrix approach developed in [39] for the scattering of electromagnetic radiation by the multilayer bianisotropic particles. In paper [36], the matrix approach has been applied to the scattering by a cloaking shell. We refer the reader to these two references for details.

According to the matrix approach, the electromagnetic field induced at the outer boundary b of the cladding (cloak) is expressed by means of the evolution operator of this layer Ω_a^b. The latter can be presented as the product of the evolution operators of each homogeneous layer $a_n < r < a_{n-1}$ ($n = 0, \ldots, N$, $a = a_0$, $b = a_N$):

$$\Omega_a^b = \Omega_{a_{N-1}}^b \Omega_{a_{N-2}}^{a_{N-1}} \ldots \Omega_a^{a_1}, \tag{A.1}$$

where N is the number of layers. The evolution operators of the homogeneous layers can be written in the analytic form and Ω_a^b can be computed.

Then the boundary conditions are solved and the scattered magnetic fields at the outer boundary b of the cladding are determined. Thus the scattering problem can be solved, because we can further obtain the near fields or far fields in terms of the scattered magnetic field. The far fields can be characterized by the differential scattering cross-sections (θ is the scattering angle) normalized by the geometrical cross-section $\sigma_g = \pi b^2$

$$D(\theta) = \frac{\mathrm{d}\sigma}{\sigma_g \sin\theta \, \mathrm{d}\theta} \tag{A.2}$$

or total scattering cross-sections

$$\sigma = \int_0^{2\pi} D(\theta) \sin\theta \, \mathrm{d}\theta. \tag{A.3}$$

References

[1] Pendry J B, Schurig D and Smith D R 2006 *Science* **312** 1780

[2] Leonhardt U 2006 *Science* **312** 1777

[3] Schurig D, Mock J J, Justice B J, Cummer S A, Pendry J B, Starr A F and Smith D R 2006 *Science* **314** 977

[4] Liu R, Ji C, Mock J J, Chin J Y, Cui T J and Smith D R 2009 *Science* **323** 366–9

[5] Leonhardt U 2006 *New J. Phys.* **8** 118

[6] Miller D A B 2006 *Opt. Express* **14** 12457

[7] Schurig D, Pendry J B and Smith D R 2006 *Opt. Express* **14** 9794
[8] Nicorovici N A P, Milton G W, McPhedran R C and Botten L C 2007 *Opt. Express* **15** 6314
[9] Liang Z X, Yao P J, Sun X W and Jiang X Y 2008 *Appl. Phys. Lett.* **92** 131118
[10] Zhao Y, Argyropoulos C and Hao Y 2008 *Opt. Express* **16** 6717
[11] Cai W S, Chettiar U K, Kildishev A V and Shalaev V M 2007 *Nat. Photonics* **1** 224
[12] Cai W S, Chettiar U K, Kildishev A V and Shalaev V M 2008 *Opt. Express* **16** 5444
[13] Vanbesien O, Fabre N, Melique X and Lippens D 2008 *Appl. Opt.* **47** 1358
[14] Xiao D and Johnson H T 2008 *Opt. Lett.* **33** 860
[15] Jenkins A 2008 *Nat. Photonics* **2** 270
[16] Valentine J, Li J, Zentgraf T, Bartal G and Zhang X 2009 *Nat. Mater.* **8** 568
[17] Milton G W, Briane M and Willis J R 2006 *New J. Phys.* **8** 248
[18] Farhat M, Guenneau S, Enoch S and Movchan A B 2009 *Phys. Rev.* B **79** 033102
[19] Zhang S, Genov D A, Sun C and Zhang X 2008 *Phys. Rev. Lett.* **100** 123002
[20] Greenleaf A, Kurylev Y, Lassas M and Uhlmann G 2008 *Phys. Rev. Lett.* **101** 220404
[21] Chen H and Chan C T 2007 *Appl. Phys. Lett.* **91** 183518
[22] Cummer S A and Schurig D 2007 *New J. Phys.* **9** 45
[23] Cai L W and Sanchez-Dehesa J 2007 *New J. Phys.* **9** 450
[24] Cummer S A, Popa B I, Schurig D, Smith D R, Pendry J, Rahm M and Starr A 2008 *Phys. Rev. Lett.* **100** 024301
[25] Greenleaf A, Lassas M and Uhlmann G 2003 *Physiol. Meas.* **24** 413
[26] Chen H, Wu B I, Zhang B and Kong J A 2007 *Phys. Rev. Lett.* **99** 063903
[27] Zhang B, Chen H, Wu B I and Kong J A 2008 *Phys. Rev. Lett.* **100** 063904
[28] Gao L, Fung T H, Yu K W and Qiu C W 2008 *Phys. Rev.* E **78** 046609
[29] Ni Y X, Gao L and Qiu C W 2009 arXiv:0905.1503 [physics.optics]
[30] Alu A and Engheta N 2007 *Opt. Express* **15** 3318
[31] Kwon D and Werner D H 2008 *Appl. Phys. Lett.* **92** 013505
[32] Jiang W X, Cui T J, Yu G X, Lin X Q, Cheng Q and Chin J Y 2008 *J. Phys. D: Appl. Phys.* **41** 085504
[33] Nicolet A, Zolla F and Guenneau S 2008 *Opt. Lett.* **33** 1584
[34] Qiu C W, Li L W, Yeo T S and Zouhdi S 2007 *Phys. Rev.* E **75** 026609
[35] Qiu C W, Hu L, Xu X and Feng Y 2009 *Phys. Rev.* E **79** 047602
[36] Qiu C W, Novitsky A, Ma H and Qu S 2009 *Phys. Rev.* E **80** 016604 (arXiv:0905.1703 [physics.optics])
[37] Dolin L S 1961 *Isvestiya Vusov* **4** 964
[38] Leonhardt U and Philbin T G 2009 *Prog. Opt.* **53** 70 (arXiv:0805.4778)
[39] Novitsky A and Barkovsky L 2008 *Phys. Rev.* A **77** 033849